Nanoscale Confinement and Temperature Effects on Associative Polymers in Thin Films: Fluorescence Study of a Telechelic, Pyrene-Labeled Poly(dimethylsiloxane)

Sung Dug Kim[†] and John M. Torkelson*[,†,‡]

Department of Chemical Engineering, and Department of Materials Science and Engineering, Northwestern University, Evanston, Illinois 60208-3120

Received January 8, 2002

ABSTRACT: This study is the first to report on the tunability of associative polymer behavior via confinement and to model the effect against experimental data. A telechelic, associative polymer, α,ω-pyrene-end-labeled poly(dimethylsiloxane) (Py−PDMS−Py), was synthesized and studied via fluorescence spectroscopy in solution at room temperature and in the neat state as a function of confinement and temperature. Emission spectra were characterized by a ratio of excimer to monomer fluorescence intensity, I_E/I_M; excitation spectra were obtained at wavelengths characteristic of monomer and excimer emission. The spectra revealed a strong tendency for static excimer fluorescence originating from ground-state dimer or aggregate formation via pyrene−pyrene association at all concentrations of Py−PDMS−Py in polymeric or oligomeric poly(dimethylsiloxane) (PDMS). The aggregates form due to the insolubility of pyrene in PDMS. In contrast, in very dilute solution in toluene, a good solvent for both pyrene and PDMS, the low excimer fluorescence was due nearly exclusively to dynamic, intramolecular excimer formation rather than to direct excitation of ground-state dimers. A very strong dependence of I_E/I_M on film thickness was observed for neat Py−PDMS−Py, with I_E/I_M being nearly independent of film thickness at thicknesses exceeding 100 to 200 nm but decreasing by more than a factor of 40 relative to bulk at a thickness of 5 nm. The dependence of I_E/I_M on film thickness was effectively described via a two-state model. The fit of the model to experimental data leads to the conclusion that the effect of confinement on association may be explained by the presence of two interfacial or surface layers of ∼ 10 nm average thickness, each having dramatically reduced physical cross-linking relative to the rest of the film. Investigation of the effect of temperature on I_E/I_M in bulk Py−PDMS−Py found that the energy of pyrene−pyrene ground-state dimer formation is about an order of magnitude greater than thermal energy (kT), making this a model system for strongly interacting, associative polymer.

Introduction

As a class of materials, nonionomeric, associative polymers have been the subject of intense interest for more than a decade.[1−25] Much of the interest has focused on associative polymers in solution, particularly with regard to aqueous systems where intramolecular and intermolecular interactions of hydrophobic groups (sometimes referred to as "stickers") attached to hydrophilic polymers can lead to a broad range of interesting behavior. From an application standpoint, such associative polymers may be useful as viscosity modifiers and in achieving improved applied coating properties. From a basic scientific standpoint, there are many issues unresolved in developing a molecular-level understanding of the viscosity modification that can be achieved with such systems. This is due in part to the fact that many studies have yet to be done on well-defined, model systems where the sticker functionality and location on the polymer and the strength of interaction are known. While solution-state behavior has been the main focus of study of associative polymers, there has also been some investigation of the behavior of neat-state, nonionomeric, associative polymers. In particular, Stadler's seminal work[21] on the properties of a thermoreversible elastomeric network based on hydrogen-bonding interactions demonstrated that, relative to nonassociative polymers, associative polymers yield both a shift in the rubbery plateau to higher temperature and lower frequency and a broadening in the relaxation time distribution.

The effect of nanoscale confinement on the dynamics of amorphous polymers has also garnered great interest over the past decade. Much of this work has focused on how the glass transition temperature, T_g, and the breadth of dynamics near T_g are affected by film thickness. The implications of confinement effects on T_g are important in a number of applications, ranging from microelectronics to polymer nanocomposites. There have been several types of systems studied over the past decade. In 1991, Jackson and McKenna[26] reported on the effect of confinement on T_g of low molecular weight glass formers in nanoporous media, finding substantial reduction in T_g for glasses formed in pores of tens of nanometers in diameter relative to bulk glasses. Similar effects have been reported by others[27−30] for both low molecular weight and polymeric glass formers in nanoporous media. In 1993 the dewetting studies by Reiter[31] and in 1994 the ellipsometry studies by Keddie et al.[32] revealed a significant depression in T_g upon reduction in thickness below 100 nm for polystyrene films supported on substrates on which polystyrene has a strong tendency to dewet. Related results have been reported by others[33−39] using a variety of techniques; some of these studies have shown that T_g may also increase with decreasing film thickness in ultrathin polymer films as long as there are attractive interactions between the polymer segments and substrate. Dutcher and co-workers[40,41] demonstrated a dramatic reduction

* To whom correspondence should be addressed.
[†] Department of Chemical Engineering.
[‡] Department of Materials Science and Engineering.

10.1021/ma0200322 CCC: $22.00
Published on Web 06/12/2002

in T_g in freely standing polystyrene films with reduction in film thickness below 70 nm and that there is a significant molecular weight dependence of the T_g depression for molecular weights exceeding 350 000. A few groups[42−44] have also studied the effect of film thickness on the temperature dependences of the breadth and average values of α-relaxation times; these studies have generally observed a broadening of the relaxation distribution with decreasing film thickness for systems in which the ultrathin film T_g was similar to or less than that in bulk. There has also been limited study[45−58] of the impact of confinement on the phase behavior of polymer blends, demonstrating the roles of entropic inhibition, polymer substrate interactions, and mechanical effects of the substrate or superstrate on phase separation.

Despite the many recent investigations of associative polymer behavior and the impact of confinement on polymer dynamics and phase behavior, relatively little has been postulated or reported in the literature regarding the impact of confinement on associative polymers. Ruths and Granick[49] investigated the impact of both the affinity of stickers to substrate/superstrate surfaces and to each other on the tribology of confined Fomblin-Z perfluoropolyalkyl ethers. Following this work, Kuznetsov and Balazs[50] applied scaling theory to determine the equilibrium behavior of a mixture of nonfunctionalized and telechelically functionalized polymers confined between planar surfaces, with an attractive potential between the functional groups and surfaces. Kumar and Douglas[20] have very recently made the case that the dynamics of associating polymer systems are phenomenologically similar to vitrification, in that changes in temperature can lead to stickers clustering into multiplets, resulting in an abrupt increase in cluster lifetimes with a small change in temperature. They indicate that this is similar to the sharp reduction in cooperative segmental mobility and the increase in number of segments involved in cooperative motion upon cooling an amorphous polymer to T_g. Here in the present study, we draw an additional parallel between the behavior of associative polymers and glass-forming polymer systems by investigating how confinement effects, extensively studied in glass-forming systems, impact the self-association or clustering of stickers in a liquid-state, neat telechelic polymer.

The particular system under study is a model telechelic, pyrene-functionalized poly(dimethylsiloxane) (Py−PDMS−Py), similar to materials recently studied by Bright and co-workers[51,52] in investigations of the pyrene-label photophysics in supercritical CO_2 solutions. Pyrene and other aromatic labels have been used previously in studies of associating polymers;[53−62] however, for the most part, these investigations were concerned with the behavior of associative poly(ethylene glycol) or poly(ethylene oxide) in aqueous systems, with the associative character being provided by the hydrophobic pyrene or other aromatic labels. In this study, the Py−PDMS−Py behavior is characterized in several solvent environments, including toluene, in which both the polymer and label are highly soluble, and high molecular weight and oligomeric poly(dimethylsiloxane) (PDMS), in which the pyrene label is highly insoluble. The core of the study concerns the associative behavior of neat Py−PDMS−Py as a function of temperature and confinement, the former being characterized over a range exceeding 100 °C and the latter being characterized over a range from 5 nm to 1 μm. The temperature effect studies reveal that that the enthalpy of pyrene−pyrene ground-state association in the Py−PDMS−Py system is roughly an order of magnitude greater than thermal energy at room temperature. Similar to the effects of confinement on the glass transition behavior of amorphous polymers, there is dramatic change in the associative behavior of this system as film thickness is reduced below ∼100 nm. This is the first report of such an effect of confinement on associative polymer behavior. A simple model indicates that the effect of nanoscale confinement can be understood to arise from two interfacial regions (polymer−air and polymer−substrate) of ∼10 nm thickness having vastly reduced association of pyrene units as compared to the interior of the film. (This model may be considered to be a variant of a two-state model applied previously[63,64] to explain fluorescence resonance energy transfer behavior of block copolymer in a combination of free solution and micellar states.) The interpretation resulting from this model is not unlike the one by Kawana and Jones,[33] who have indicated that the effect of confinement on polymer T_g has its origins in ∼10-nm-thick interfacial regions with dynamics vastly different from those in bulk.

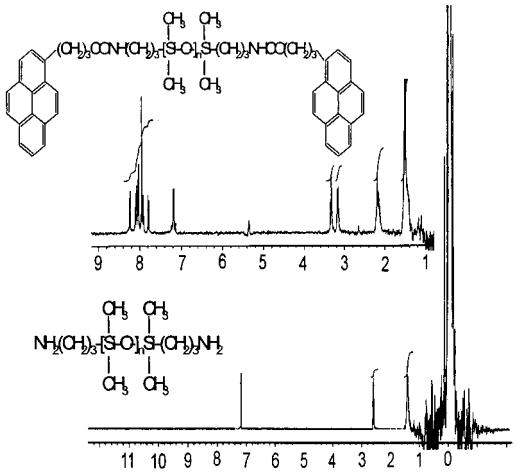

Figure 1. Proton NMR spectra of NH_2–PDMS−NH_2 (bottom) and Py−PDMS−Py (top).

Experimental Section

Materials. All materials were purchased from Aldrich and used as received unless otherwise specified. α,ω-Aminopropyl-terminated PDMS (NH_2–PDMS−NH_2) of 27 kg/mol nominal number-average molecular weight, M_n, and 2 Pa s viscosity at room temperature was used as a precursor for the pyrene end-labeled PDMS. The M_n of NH_2–PDMS−NH_2 was measured by ^{1}H nuclear magnetic resonance (NMR) spectroscopy, assuming that all PDMS chains have two amine-end groups. The peaks for CH_2NH_2 at 2.6 ppm and $SiCH_3$ at 0 ppm were integrated, yielding an estimate of M_n of 24 ± 1 kg/mol (Figure 1). NH_2–PDMS−NH_2 was reacted in tetrahydrofuran with a 4-fold molar excess of 1-pyrene butyric acid N-hydrosuccinimide ester for 1 day at room temperature. The reactant mixture was dried, and then small molecules of 1-pyrene butyric acid *N*-hydrosuccinimide ester and reaction byproducts were extracted 10 times with excess methanol. The reaction product was analyzed by NMR and gel permeation chromatography (GPC). GPC (Waters Co.), employing tetrahydrofuran as solvent, was equipped with three columns and three detectors of UV absorbance, fluorescence, and refractive index. No small molecules were found on the GPC trace of Py−PDMS−Py by the fluorescence detector with excitation wavelength of 340 nm and emission wavelength of 394 nm,

confirming that small molecules containing pyrene were washed away successfully. The molecular weight of Py−PDMS−Py was determined via GPC against polystyrene standards without further correction. Number-average molecular weight and weight-average molecular weight, M_w, were 22 kg/mol and 34 kg/mol, respectively, indicative of moderate polydispersity in the polymer. The NMR spectrum of Py−PDMS−Py shows that the peak for the unreacted amine end groups at 2.6 ppm decreases to noise level. Amide protons, $-CH_2NHCO-$, at 3.4 and 5.4 ppm and pyrene protons at 7.8−8.2 ppm are indicative of the chemical reaction between the amine group and pyrene butyric acid *N*-hydrosuccinimide ester (Figure 1). It was determined from these characteristic peaks that 91 ± 6% of the amine end groups were modified to pyrene end groups. This is consistent with previously reported results[51] showing that the reaction produced mostly Py−PDMS−Py.

Sample Preparation. Solutions of Py−PDMS−Py in toluene, octamethyltrisiloxane, or unlabeled PDMS were prepared in cuvettes with 1.0-cm path length. Films were spin-coated from hexane solutions on quartz or silicon wafers. Film thickness was obtained by ellipsometry only on films made on silicon substrates, due to the necessity of high reflection from the substrate for ellipsometric characterization. In contrast, fluorescence intensity was obtained for Py−PDMS−Py deposited only on quartz slides, due to the fact that high reflection of light from silicon wafers results in abnormal fluorescence spectrum. If the spin coating conditions such as polymer concentration and spin coating speed are identical, the resulting film thickness is the same, regardless of the substrate.[65] For thick samples, film thickness was adjusted by a spacer between quartz slides.

Steady-State Fluorescence Spectroscopy. Pyrene steady-state fluorescence spectra were measured with a SPEX Fluorolog-2 DM1B fluorimeter using a front-face geometry with 1.25 mm excitation and emission slits (band-pass = 2.5 nm). For all emission spectra, the excitation wavelength was 342 nm. For excitation spectra, which differ from emission spectra by holding the emission wavelength constant while scanning on excitation wavelength, the emission wavelength was 396 nm (480 nm) for monomer (excimer) excitation spectra. Unless otherwise specified, all fluorescence measurements were obtained at room temperature under air atmosphere. Film temperature above room temperature was varied using a flat ribbon heater mounted on a thin aluminum plate. A cuvette equipped with water jacket was used to adjust sample temperature below room temperature. The fluorescence intensity is expressed as the ratio between the sample cell and a reference cell. For ultrathin films, a spectrum of a blank quartz slide was obtained before a thin film is coated on the quartz. Then a corrected fluorescence spectrum of a thin film coated on the quartz substrate was obtained by subtracting the background spectrum of the quartz substrate from the measured spectrum of the ultrathin Py−PDMS−Py film on the quartz substrate. In almost all fluorescence measurements, background fluorescence intensity due to electronic noise and substrate is less than 10%. Further details regarding fluorescence measurements on ultrathin polymer films may be found in ref 66.

Results and Discussion

Py−PDMS−Py in Solution. Typical fluorescence spectra for solutions of Py−PDMS−Py in a good solvent, toluene, are shown in Figure 2. A highly structured emission observed at shorter wavelength is associated with fluorescence from a single excited-state pyrene unit or monomer fluorescence while the broad structureless emission at longer wavelength is associated with fluorescence from an excited-state dimer of pyrene units, also called the excimer state. Here a relative measure of interaction between pyrene end groups may be characterized by I_E/I_M, where I_E, representing the excimer intensity, is taken to be the intensity at 480 nm, and I_M, representing the monomer intensity, is taken to be the intensity at 396 nm. The presence of excimer fluorescence in solutions of Py−PDMS−Py has been previously reported by other researchers.[51,52,67]

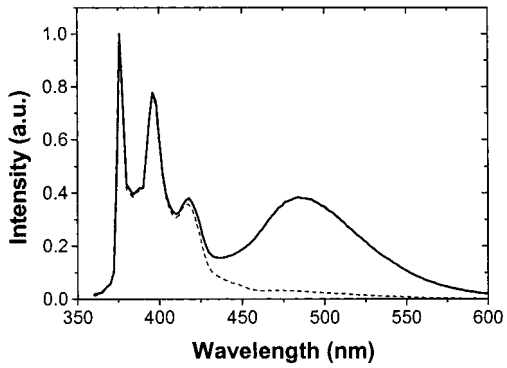

Figure 2. Fluorescence emission spectra for solutions of Py−PDMS−Py in a good solvent, toluene. The intensities of Py−PDMS−Py solutions of 10^{-4} g/mL (dashed line) and 10^{-1} g/mL (solid line) are normalized at 396 nm, indicative of monomer fluorescence.

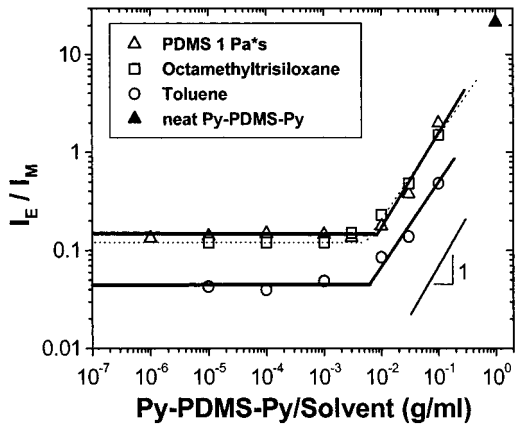

Figure 3. Excimer to monomer intensity ratio of Py−PDMS−Py in toluene, octamethyltrisiloxane, and high molecular weight PDMS. Lines are present simply to guide the eye.

Figure 3 shows I_E/I_M as a function of Py−PDMS−Py concentration for several conditions: one where Py−PDMS−Py is in toluene, a good solvent for both the PDMS main chain and the pyrene labels; a second, where Py−PDMS−Py is in octamethyltrisiloxane, which is expected to be a good solvent for the PDMS main chain but a poor solvent for the pyrene labels; and a third, where Py−PDMS−Py is in unlabeled PDMS, which should have solvent quality comparable to that of octamethyltrisiloxane but a much higher viscosity (1 Pa s vs 0.001 Pa s). Under very dilute conditions, I_E/I_M is independent of concentration, since each polymer is spatially separated, meaning that pyrene−pyrene interaction is determined by local pyrene concentration rather than the overall pyrene concentration in solution. In very dilute toluene solution, it is expected that interaction between pyrene groups should be nearly exclusively intramolecular and dynamic in nature, leading to I_E/I_M values that are independent of polymer concentration.[54,68] Such a result is obtained, as shown in Figure 3. However, while I_E/I_M remains independent of concentration in very dilute solution of Py−PDMS−Py in octamethyltrisiloxane, the value of I_E/I_M is significantly higher than that obtained from toluene solutions. Even more striking is the fact that values of

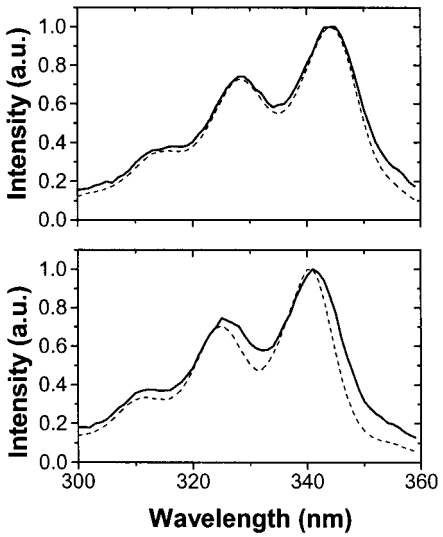

Figure 4. Excitation spectrum of 10^{-4} g/mL solution of Py−PDMS−Py in toluene (top) and octamethyltrisiloxane (bottom) monitored at monomer emission wavelength, 396 nm (dashed line), and excimer emission wavelength, 480 nm (solid line).

I_E/I_M are almost identical for octamethyltrisiloxane and PDMS solutions.

These results may be explained as follows. In the case of dilute solution in toluene, almost all excimer formation is intramolecular and dynamic in nature. The dynamic nature is confirmed by measurement of excitation spectra at two emission wavelengths, one characteristic of monomer fluorescence (396 nm) and the second characteristic of excimer fluorescence (480 nm). See Figure 4. For very dilute solution of Py−PDMS−Py in toluene, the two excitation spectra are identical within error, indicating that essentially all excimer fluorescence originates with excited-state monomer and results from the formation of excimer by dynamic interaction of a second ground-state pyrene unit with the excited-state pyrene monomer during its excited-state lifetime. In the case of very dilute solutions of Py−PDMS−Py in octamethyltrisiloxane or PDMS, the independence of I_E/I_M with concentration indicates that excimer formation is also intramolecular in nature. However, the higher values of I_E/I_M as compared to that in toluene and the near independence of the intensity ratio with solvent viscosity (octamethyltrisiloxane vs PDMS) suggest that a significant portion of excimer formation in the silicon-based solvents is static in nature, i.e., originating from direct excitation of ground-state dimers resulting from pyrene unit aggregation. The presence of ground-state dimers or aggregates is confirmed by excitation spectra measurements in Figure 4, which show substantial broadening in the excimer excitation spectrum relative to that of the monomer excitation spectrum for octamethyltrisiloxane solutions. (A good review of the use of excitation spectra for distinguishing the presence of static excimer formation via ground-state dimers from dynamic excimer formation is found in ref 69.) Table 1 compares peak wavelengths and valley to peak intensity ratios from the excitation spectra. For all solvent systems, peak and valley locations are identical within experimental error. However, in the case of the octamethyltrisiloxane and PDMS solvent systems, there is a substantial increase in I_{valley}/I_{peak} at the 480 nm observation wavelength relative to that at the 396 nm observation wavelength, indicative of peak broadening in the excimer excitation spectra. The broadening of the peaks clearly indicates that Py−PDMS−Py in octamethyltrisiloxane and highly viscous PDMS undergoes intramolecular, ground-state aggregation. The formation of ground-state dimers in the two silicon-based solvents is not unexpected, given that pyrene is not well-dissolved in these systems and that it has been previously reported that phase separation between solvent and pyrene labels on a polymer in solution can cause pyrene to form static excimers or ground-state dimers.[54,62,68,70]

Table 1. Characteristics of Excitation Spectra of 10^{-4} g/mL Py−PDMS−Py in Toluene, Octamethyltrisiloxane, and PDMS with a Viscosity of 1 Pa s

solvent	observation wavelength (nm)	peak position (nm)	valley position (nm)	valley to peak intensity ratio I_{valley}/I_{peak}
toluene	396	344	335	0.55
toluene	480	345	334	0.58
octamethyltrisiloxane	396	341	331	0.48
octamethyltrisiloxane	480	341	332	0.58
1 Pa s PDMS	396	341	332	0.45
1 Pa s PDMS	480	342	333	0.57

In addition, hydrogen bonding between the amide hydrogen at one chain end to the carbonyl residue at the other end of the same Py−PDMS−Py chain may enhance the ground-state dimer formation. Farinha et al.[71] studied pyrene-end-labeled polystyrene in cyclohexane, where pyrene is chemically linked to polystyrene through an amide bond. They found that pyrene-terminated polystyrene exhibited ground-state excimer formation and argued that hydrogen bonding causes the ground-state excimer. In contrast, Kane et al.[51] studied Py−PDMS−Py in toluene (10 μM pyrene group concentration that corresponds to 2.4×10^{-4} g/mL in our system), confirming the absence of ground-state dimer. They speculated that the high flexibility of the PDMS chain and/or the fact that toluene is a good solvent for PDMS significantly decreased or eliminated hydrogen bonding between amide groups on the pyrene end units in Py−PDMS−Py.

The excimer to monomer intensity ratio data in Figure 3 can be divided into two regimes: a plateau regime in very dilute concentration and a concentration-dependent regime at higher concentration. In the concentration-dependent regime, I_E/I_M is approximately linearly proportional to concentration. Char et al.[54] studied α,ω-pyrene-labeled poly(ethylene glycol) in a water/methanol system and also found that intermolecular interactions of pyrene in concentrated solutions resulted in I_E/I_M scaling linearly with the pyrene concentration. On the basis of the results in Figure 3 for all three Py−PDMS−Py systems, the transition concentration between the plateau regime and the concentration-dependent regime is $\sim 5 \times 10^{-3}$ to 1×10^{-2} g/mL. At concentrations exceeding this transition concentration, polymer chains interact with other polymer chains in solution, leading to significant intermolecular excimer formation. According to polymer solution theory,[72] a typical noninteractive polymer in solution shows a critical concentration, c^*, at which the chains begin to overlap. The value of c^* can be theoretically estimated from the intrinsic viscosity of the polymer by use of the equation $c^* = A[\eta]^{-1}$, where A may take on values on the order of 1.[73] However, the transition concentration in Figure 3 is an order of magnitude lower than c^* estimated from the literature values[74] of intrinsic viscosity of PDMS. For 24 kg/mol molecular weight

Table 2. Characteristics of Excitation Spectra of Neat Py−PDMS−Py as a Function of Temperature[a]

temp (°C)	$\Delta\lambda$ (nm)	$(I_{valley}/I_{peak})_{480}/(I_{valley}/I_{peak})_{396}$
22	3	1.85
60	3	1.59
100	2	1.26
140	1	1.08

[a] $\Delta\lambda$ represents the wavelength difference of peaks monitored at 480 and 396 nm emission wavelength. Values $(I_{valley}/I_{peak})_{480}$ and $(I_{valley}/I_{peak})_{396}$ represent valley to peak intensity ratio monitored at 480 and 396 nm emission wavelength, respectively.

PDMS, $[\eta]^{-1}$ values are estimated to range from 7.0×10^{-2} to 9.5×10^{-2} g/mL, depending on whether the solvent is a θ-solvent or good solvent for PDMS. The fact that the transition concentration in Figure 3 is considerably lower than estimated c^* values indicates that Py−PDMS−Py solutions differ significantly from noninteractive polymer solutions. In particular, attractive interactions between pyrene labels may induce observable intermolecular interaction between Py−PDMS−Py molecules at concentrations significantly below the theoretical overlap concentration, especially if the lifetime of the transient pyrene aggregates is substantial.

Figure 3 reveals that in the neat state Py−PDMS−Py exhibits a value of I_E/I_M that is more than 2 orders of magnitude higher than I_E/I_M in dilute toluene solution. Additionally, Tables 1 and 2 reveal that while the excitation spectrum of Py−PDMS−Py in very dilute solution in octamethyltrisiloxane or PDMS exhibits almost no shift in peak maximum and some spectral broadening with emission wavelength, the excitation spectrum of neat Py−PDMS−Py observed at 480 nm is much broader and red-shifted by 3 nm relative to the excitation spectrum observed at 396 nm. The very high I_E/I_M value and the excitation spectra for neat Py−PDMS−Py indicate that most pyrene end groups are associated in ground-state aggregate structures. This ground-state aggregation of pyrene end groups has great impact on the physical properties of neat Py−PDMS−Py. For example, at room temperature, neat Py−PDMS−Py has a viscosity that is ∼20 times higher than that of neat NH_2−PDMS−NH_2 with the same molecular weight of 24 kg/mol. The Py−PDMS−Py also shows a dramatic increase in viscosity with decreasing temperature and forms gels at ∼10 °C.[75] As a consequence, it is believed that pyrene aggregation in Py−PDMS−Py results in physical cross-linking having the nature of a transient network rather than that of permanent cross-linking. The sections that follow describe the impact of confinement and temperature on the degree of physical cross-linking and related properties of the Py−PDMS−Py in the neat state.

Confinement Effects on Thin Films of Neat Py−PDMS−Py. In the general case, the overall shape of the fluorescence spectrum of a photophysical probe or label does not depend on polymer film thickness.[66] In other words, normalized spectra should generally be the same at all film thicknesses. However, fluorescence measurements from neat Py−PDMS−Py show that the normalized fluorescence spectrum is a significant function of film thickness in ultrathin films. This is evident from the results in Figure 5, where the ratio of excimer to monomer fluorescence intensity is seen to be significantly reduced in a 44-nm-thick film relative to that in a 242-nm-thick film. Furthermore, the high sensitivity

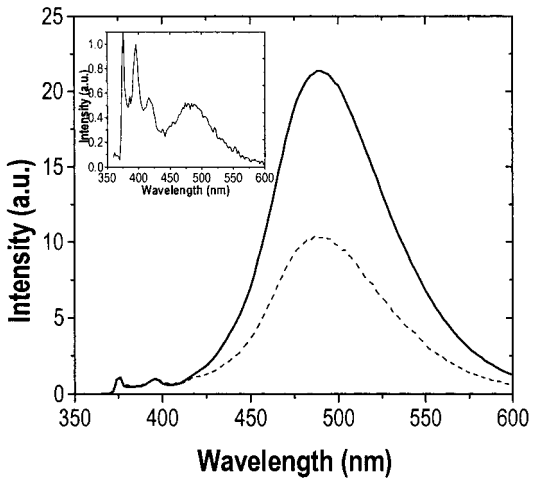

Figure 5. Fluorescence emission spectrum of neat Py−PDMS−Py in thin and ultrathin films. The intensities of a 242-nm-thick film (solid line) and a 44-nm-thick film (dashed line) are normalized at 396 nm. Inset shows the normalized emission spectrum of a 5-nm-thick film.

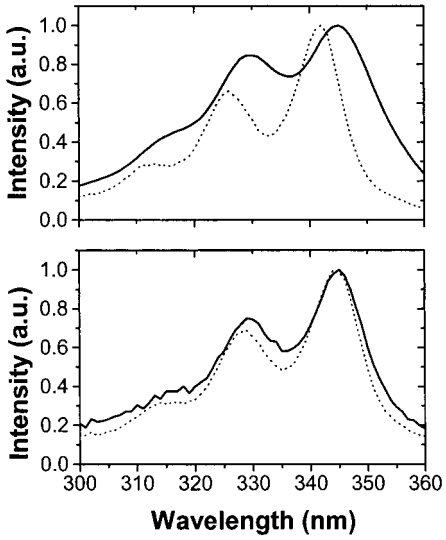

Figure 6. Excitation spectrum of Py−PDMS−Py films with a thicknesses of 390 nm (top) and 5 nm (bottom) monitored at monomer emission wavelength, 396 nm (dashed line), and excimer emission wavelength, 480 nm (solid line).

of fluorescence spectroscopy produces easily resolvable and well-defined monomer peaks and a broad excimer peak for ultrathin films as thin as 5 nm. With the 5-nm-thick film, the value of I_E/I_M is found to be 0.5, nearly 2 orders of magnitude lower than that in the 242-nm-thick film.

Excitation spectra shown in Figure 6 provide further insight into the effect of confinement on pyrene−pyrene interactions in ultrathin Py−PDMS−Py films. For a 390-nm-thick film, the excitation spectrum observed at 480 nm is much broader and red-shifted by 3 nm relative to that observed at a 396-nm emission wavelength, indicating that pyrene end groups are aggregated. In contrast, the excitation spectrum of a 5-nm-thick film measured at a 480-nm emission wavelength shows no red-shift and little spectral broadening as compared to the excitation spectrum at a 396-nm emission wavelength, indicating that pyrene−pyrene aggregation or physical cross-linking is nearly absent at this film thickness. The Py−PDMS−Py excitation spectra provide ample evidence that confinement in-

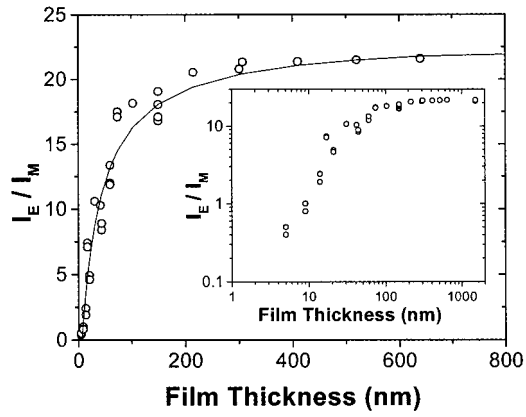

Figure 7. Excimer to monomer intensity ratio of neat Py−PDMS−Py as a function of film thickness. The curve is a nonlinear fit to eq 1. Inset shows log(I_E/I_M) vs log(film thickness).

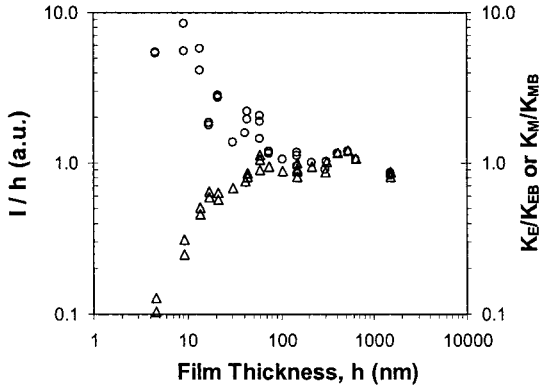

Figure 8. Intensity divided by film thickness, I/h, of monomer (circles) and excimer (triangles) fluorescence. I/h values are normalized against respective I/h values in bulk. Average I/h values of monomer and excimer in films with thickness above 300 nm are taken as I/h in bulk. Note that $K_E/K_{EB} = I_E/h$ (normalized to bulk) and $K_M/K_{MB} = I_M/h$ (normalized to bulk). K_E/K_{EB} and K_M/K_{MB} are parameters used in eq 1.

duces substantial differences in the network structure between bulk and ultrathin films.

Figure 7 shows I_E/I_M as a function of film thickness from 5 nm to more than 1 μm. The intensity ratio is essentially independent of thickness for film thickness greater than 200 nm. Thus, the network structure of Py−PDMS−Py in films of thickness greater than 200 nm is believed to be identical to that of bulk Py−PDMS−Py. However, I_E/I_M is reduced with decreasing film thickness below 200 nm, and the effect is particularly dramatic for thickness below 100 nm. These measurements along with the measurements of excitation spectra clearly demonstrate that confinement greatly reduces the extent of aggregation and physical crosslinking in the associative Py−PDMS−Py system.

Previous research[66] has shown that the fluorescence intensity, I, of a pyrene probe or label at low, constant concentration in thin films of glassy polymer is linearly proportional to the film thickness h, when absorbance is less than 0.05, and that within error all fluorescence is monomer in origin with no excimer being evident. That is, the emission intensity divided by film thickness is the same for all film thicknesses: $I/h = K$. In contrast, Py−PDMS−Py films have fluorescence behavior much different from pyrene in glassy polymers. Figure 8 shows normalized monomer intensity divided by film thickness, I_M/h, and normalized excimer intensity divided by film thickness, I_E/h, as functions of film thickness. Alternatively, values of K_M/K_{MB} and K_M/K_{MB} represent respective proportionality constants for monomer and excimer, K_M and K_E, divided by corresponding bulk values, K_{MB} and K_{EB}. Values of I_M/h and I_E/h are nearly constant for films thicker than 100 nm, as expected. However, for films thinner than 100 nm, I_E/h decreases dramatically with decreasing film thickness while I_M/h increases sharply with decreasing film thickness. This may be understood to arise from the fact that pyrene aggregation is reduced and more pyrene monomer is present in thinner films.

The overall shape of the relationship between I_E/I_M and film thickness as shown in Figure 7 resembles a typical isotherm curve, suggesting that the relationship may be explained via a simple two-state model. (Likewise, the inset plot in Figure 7 demonstrates an approximate power-law relationship between I_E/I_M and film thickness over the range where the intensity ratio is dependent on thickness.) It is noteworthy that the shape of the curve in Figure 7 also resembles that obtained by Keddie et al.[32] when they determined the impact of confinement on T_g of polystyrene films. Jones developed an empirical model describing T_g reduction with decreasing film thickness that basically divided the film into two states or regions: bulk and surface layer. A fit of the model to experimental data[33,76] leads to the conclusion that a surface layer with liquidlike properties and high mobility, distinct in dynamics from that of the rest of the film, has a thickness on the order of 10 nm.

In our simple two-state model for explaining the Py−PDMS−Py film thickness dependence of I_E/I_M, a film is assumed to consist of one interior layer possessing bulk behavior and two interface layers at the polymer−air and polymer−substrate interfaces. Since we do not have a method to distinguish between these interface layers, they are treated here as identical layers (or equivalently with an average interfacial behavior) with the same thickness. Our model assumes that overall monomer fluorescence is a sum of that from the interior or bulk layer and two interfacial layers and that a similar sum applies to overall excimer fluorescence:

$$\frac{I_E}{I_M} = \frac{K_{EB}h_B + 2K_{EI}h_I}{K_{MB}h_B + 2K_{MI}h_I} = \frac{K_{EB}h + 2(K_{EI} - K_{EB})h_I}{K_{MB}h + 2(K_{MI} - K_{MB})h_I} = \frac{hK_{EB}/K_{MB} + a}{h + b} \quad (1)$$

where I and K are fluorescence intensity and proportionality constants, respectively. The parameters h, h_B, and h_I are the thicknesses of the entire film, bulk, and interfaces ($h = h_B + 2h_I$), respectively. (This also means that eq 1 is strictly valid only for $h > 2h_I$) The subscripts E and M represent excimer and monomer, respectively, whereas subscripts B and I represent bulk and interface, respectively. A nonlinear fit based on eq 1 of the data in Figure 7 produces $K_{EB}/K_{MB} = 23.2 \pm 0.7$, $a = -139 \pm 28$, $b = 35.5 \pm 6.0$.

Beyond the reasonable agreement of this simple model to the data, the values of a and b obtained from the fit are also noteworthy, as they describe the fluorescence properties in the pure interface and can be used to estimate the interfacial thickness. If a film is com-

prised of only two interfaces and no interior layer, then the values of K_{EI}/K_{EB} and K_{MI}/K_{MB} are identical to the values of K_E/K_{EB} and K_M/K_{MB} shown in Figure 8. (For example, for a 31-nm-thick film, $h_I = 16.5$ nm and K_{EI}/K_{EB} and K_{MI}/K_{MB} are 0.68 and 1.4, respectively.) From simple arguments,[77] $a = 2h_I(K_{EB}/K_{MB})(K_{EI}/K_{EB} - 1)$. Using data from Figure 8, the calculated values of a using the equation immediately above most closely approximates the value of a obtained from the nonlinear fit of eq 1 to the data in Figure 7 when $2h_I = 17$ nm. Similarly, $b = 2h_I(K_{MI}/K_{MB} - 1)$. Values of K_{MI}/K_{MB} may be taken from Figure 8, and the calculated values of b using these data most closely agree with the value of b obtained from the nonlinear fit of eq 1 to the data in Figure 7 when $2h_I = 21$ nm. These values imply that each interfacial layer, with dramatically reduced pyrene unit aggregation relative to bulk, is ~10 nm thick. This result is strikingly similar to the result by Jones[33,76] indicating that the dependence of T_g on the thickness of ultrathin polymer films may be explained by a surface layer of ~10 nm thickness with dynamics dramatically different from that of the film interior.

While the quantitative relationship between associative polymer behavior as manifested by I_E/I_M and film thickness may be rationalized by the two-state model, the underlying molecular or segmental scale cause of the effect of confinement on association is an open question and merits further study. This is yet another parallel with the effect of confinement on glass transition behavior in ultrathin films where much work is currently ongoing in order to determine its molecular or segmental level origins. There are several issues related to the molecular scale origin of the tunability of associative polymer behavior via confinement that deserve further study. These include the following: the extent to which sticker segregation to or from the surface/interfacial regions may be present and the impacts of steric restrictions on sticker aggregation and of reduced polymer chain conformational possibilities in the several-nanometer-thick surface/interfacial regions. It is also possible that the magnitude of the confinement effect may be related to the overall strength of the sticker interaction, just as the effect of confinement on T_g has been correlated to the strength of interactions between polymer repeat units and substrate.[32,33,36,39] While the present study does not undertake a variation in the overall strength of the sticker interaction, it does provide a measure of the relative strength of the sticker interaction through characterization of the effect of temperature on the fluorescence of neat Py−PDMS−Py, which is described below.

Temperature Effect on Excimer to Monomer Intensity Ratio of Neat Py−PDMS−Py. Figure 9 shows I_E/I_M for bulk Py−PDMS−Py as a function of temperature. The circles represent data obtained upon heating, while the triangles represent data taken upon cooling. With increasing temperature, I_E/I_M decreases, indicating that the extent of physical cross-linking is reduced at higher temperature. The fluorescence data taken upon cooling agree well with the data taken upon heating. Therefore, the fluorescence response, and hence the physical cross-linking, of the Py−PDMS−Py is thermoreversible. The lack of hysteresis in the fluorescence response may be ascribed to the fast segmental motion of the PDMS backbone at the temperature range under study as well as the transient nature of the physical cross-links in Py−PDMS−Py.

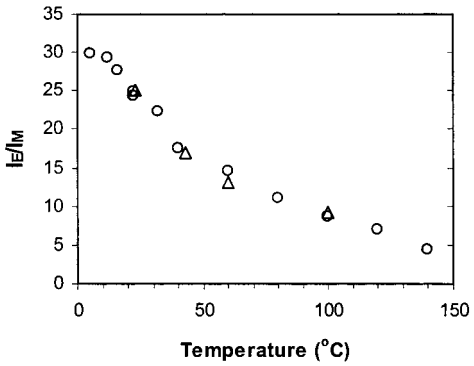

Figure 9. Effect of temperature on excimer to monomer intensity ratio in bulk Py−PDMS−Py. A fluorescence spectrum was recorded, and each subsequent measurement was taken 5 min after the sample had been heated (circles) or cooled (triangles) to the next temperature setting.

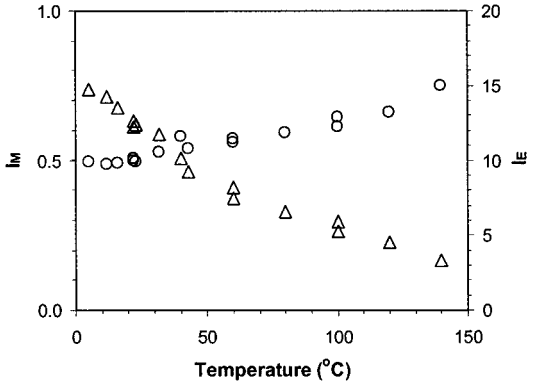

Figure 10. Effect of temperature on monomer intensity (I_M, circles) and excimer intensity (I_E, triangles) of bulk Py−PDMS−Py.

Figure 10 shows monomer intensity and excimer intensity as functions of temperature. Excimer intensity decreases with increasing temperature, which is not unusual since chromophore fluorescence intensity typically decreases with increasing temperature. The "temperature quenching effect"[78] describes the decrease in the fluorescence intensity at higher temperature due to the higher mobility of molecules and more frequent collision between molecules, which brings the electrons in the excited state to the ground state through nonradiative processes. However, the increase in monomer intensity with increasing temperature that is shown in Figure 10 cannot be explained by a temperature quenching effect. Instead, the temperature dependence of the equilibrium between pyrene monomer and aggregate is the origin of the increase in monomer intensity with higher temperature. Excitation spectra provide information regarding the pyrene−pyrene interaction as a function of temperature. Table 2 summarizes the characteristics of the excitation spectrum at temperatures ranging from 22 to 140 °C. At 22 °C, the excitation spectrum monitored at 480 nm is red-shifted and has a high valley to peak intensity ratio with respect to that monitored at 396 nm. With increasing temperature, the degree of pyrene aggregation decreases, which is evident from the smaller peak shift and the lower relative valley to peak intensity ratio. However, even at 140 °C, there is a noticeable difference between the excitation spectra monitored at 480 and 396 nm, indicating the presence of pyrene aggregation. As a result, it is expected that the association energy of pyrene−pyrene aggregation in

neat Py−PDMS−Py is significantly higher than thermal energy at room temperature.

The temperature dependence of both monomer and excimer intensities may be used to estimate the pyrene−pyrene association energy in the ground state, ΔH_A. Assuming an equilibrium between monomer, M, and ground-state dimer, D, then the equilibrium constant K_{eq} is equal to $[D]/[M]^2$, where [D] represents the ground-state dimer concentration and [M] represents the monomer concentration. This simple equilibrium model is based on the fact that pyrene crystal consists of dimer structure.[79] Here the level of dynamic excimer is assumed to be much smaller than the ground-state dimer as indicated from the excitation spectra of bulk Py−PDMS−Py under such circumstances. The monomer intensity and excimer intensity should then be approximately proportional to [M] and [D], respectively,

$$K_{eq} = [D]/[M]^2 = kI_E/I_M{}^2 \quad (2)$$

where k is a proportionality constant.

The fluorescence intensity change as a function of temperature originates from two factors, first from the change of [D] and [M] and second from the temperature quenching effect. The temperature quenching effect should be subtracted to determine the equilibrium constant in eq 2. To estimate the temperature quenching effect, the fluorescence intensities of the model compounds pyrene and 1-pyrene butyric acid *N*-hydrosuccinimide ester, in PDMS, were measured as functions of temperature. At extremely low chromophore concentration, 10^{-6} g/mL, pyrene is found to exist in the monomer state with negligible dimer. As expected, the monomer fluorescence intensity at pyrene concentration of 10^{-6} g/mL decreases with increasing temperature due to the temperature quenching effect. The effect of temperature on the monomer intensities of the two model compounds was analyzed by an Arrhenius plot. Pyrene and 1-pyrene butyric acid *N*-hydrosuccinimide in PDMS yielded the same apparent activation energy of 6.3 kJ/mol ($R^2 > 0.99$). This activation energy was used to obtain corrected fluorescence intensities of monomer and excimer of neat Py−PDMS−Py, which are proportional to the "true" concentrations of [M] and [D]. Having corrected for the temperature quenching effect on fluorescence intensities, the parameter k in eq 2 can be treated as a constant.

Combined with eq 2, the van't Hoff plot of $K_{eq} = \exp(-\Delta H_A/RT + \Delta S/R)$ provides a way to estimate the enthalpy of ground-state dimer formation. As determined from Figure 11, this association energy of pyrene−pyrene aggregation in the ground-state is estimated to be −21 kJ/mol, an order of magnitude greater in absolute value than the associated thermal energy at room temperature ($kT \sim 2.4$ kJ/mol at room temperature). The absolute value of the pyrene−pyrene association energy is also within the range (middle to upper end) of activation energy values commonly reported for hydrogen bonds.[80−82]

This high absolute value for the enthalpy of pyrene−pyrene association indicates that there should be a high propensity for pyrene units to be in associated structures or aggregates in Py−PDMS−Py systems and thus explains both the intramolecular and intermolecular aggregation between chain ends in Py−PDMS−Py. The high absolute value of the enthalpy of pyrene−pyrene association in these systems also suggests that the lifetime of the aggregates in these transient networks may be relatively long,[83] consistent with both the observation of interpolymer pyrene−pyrene association in solution at concentrations well below c^* and limited results obtained in studies of Py−PDMS−Py rheological response. Details of the unusual rheological properties of the Py−PDMS−Py and effects of confinement on the phase behavior of thin film blends of Py−PDMS−Py and NH_2−PDMS−NH_2 are reported elsewhere.[48,75]

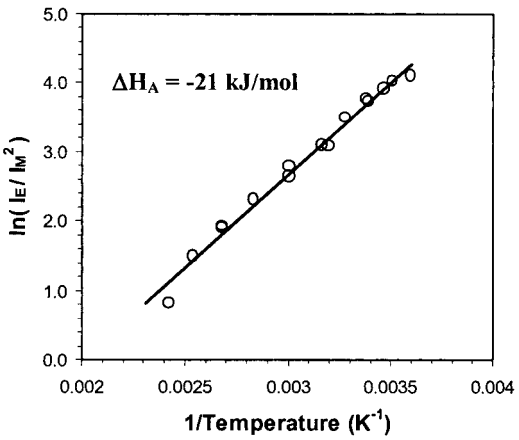

Figure 11. van't Hoff plot of fluorescence data for bulk Py−PDMS−Py allowing a determination of ground-state pyrene−pyrene association energy, ΔH_A. $\Delta H_A = -21$ kJ/mol ($R^2 = 0.99$) from linear regression analysis.

Conclusions

Telechelic, pyrene-labeled PDMS was found to provide an excellent model system for investigating associative polymer behavior in solution and in the neat state as a function of temperature and confinement. The choice of pyrene as the sticker was particularly useful in that pyrene was not only responsible for the associative behavior but also because the state of association could be directly investigated via measurement of fluorescence from the pyrene labels. From a combination of fluorescence emission and excitation spectra, it was possible to comment on the presence of ground-state dimer formation, responsible for static excimer fluorescence and which is correlated to the associative response of the polymer, relative to that of dynamic excimer formation and monomer fluorescence.

Associative behavior of Py−PDMS−Py in solution in oligomeric and polymeric PDMS, in which pyrene is very insoluble, is observed over a very broad range of concentration, including extremely dilute solutions where the presence of ground-state dimer formation between pyrene units is strictly intramolecular. Only in very dilute solutions in toluene, a good solvent for both pyrene and PDMS, is there a negligible level of pyrene aggregation, as evidenced by the low level of excimer fluorescence being associated with dynamic rather than static excimers. Due to the relatively strong pyrene−pyrene aggregation energy, which may be correlated with a relatively long lifetime of the transient pyrene aggregates, intermolecular aggregate formation can be observed at concentrations of Py−PDMS−Py well below that of the theoretical overlap concentration, c^*, at which interpolymer interaction of nonassociative polymers in solution becomes evident. The enthalpy of pyrene−pyrene aggregation was quantified by analysis of fluorescence behavior of bulk Py−PDMS−Py, reveal-

ing it to be nearly 1 order of magnitude greater in absolute value than thermal energy.

In bulk Py−PDMS−Py, I_E/I_M is more than 2 orders of magnitude greater than that found in very dilute solution, with strong evidence that the excimer fluorescence is dominated by static rather than dynamic excimers. However, confinement greatly affects values of I_E/I_M when film thickness is less than 100−200 nm. At a film thickness of 5 nm, I_E/I_M is more than a factor of 40 smaller than the value in bulk. The relationship of I_E/I_M to film thickness can be determined quantitatively via a two-state model, resulting in the conclusion that interfacial regions of ∼10 nm thickness have dramatically reduced excimer fluorescence and physical cross-linking relative to the interior portion of the film. Comparison of excitation spectra taken in bulk Py−PDMS−Py and ultrathin Py−PDMS−Py films further supports the notion that aggregation is greatly reduced in ultrathin films. The conclusion that confinement effects may be explained by interfacial regions of ∼10 nm thickness which have dramatically reduced associative behavior relative to bulk is similar to a recent explanation of the origin of the strong effect of confinement on the glass transition behavior of ultrathin films. This is the first report of dramatic effects of confinement on associative polymer behavior, and as such, the underlying molecular or segmental level origins of the impact of confinement on associative behavior are not yet known; future experimental and theoretical studies will be needed to determine these origins. However, the results presented here make clear that associative polymer behavior, such as physical gelation, which has been long understood to be tunable via temperature, is also tunable via confinment.

References and Notes

(1) Balazs, A. C.; Hu, J. Y. *Langmuir* **1989**, *5*, 1253.
(2) Santore, M. M.; Russel, W. B.; Prud'homme, R. K. *Macromolecules* **1989**, *22*, 1317.
(3) Lundberg, D. J.; Glass, J. E.; Eley, R. R. *J. Rheol.* **1991**, *35*, 1255.
(4) Leibler, L.; Rubinstein, M.; Colby, R. H. *Macromolecules* **1991**, *24*, 4701.
(5) Ezzell, S. A.; McCormick, C. L *Macromolecules* **1992**, *25*, 1887.
(6) Zhang, Y. X.; Da, A. H.; Butler, G. B.; Hogenesch, T. E. *J. Polym. Sci. Part A: Polym. Chem.* **1992**, *30*, 1383.
(7) Yekta, A.; Duhamel, J.; Brochard, P.; Adiwidjaja, H.; Winnik, M. A. *Macromolecules* **1993**, *26*, 1829.
(8) Persson, K.; Wang, G.; Olofsson, G. *J. Chem. Soc., Faraday Trans.* **1994**, *90*, 3555.
(9) Alami, E.; Almgren, M.; Brown, W.; Francois, J. *Macromolecules* **1996**, *29*, 2229.
(10) English, R. J.; Gulati, H. S.; Jenkins, R. D.; Khan, S. A. *J. Rheol.* **1997**, *41*, 427.
(11) Xu, B.; Yekta, A.; Li, L. Masoumi, Z. Winnik, M. A. *Colloid Surf. A* **1996**, *112*, 239.
(12) Rubinstein, M.; Dobrynin, A. V. *Trends Polym. Sci.* **1997**, *5*, 181.
(13) Tam, K. C., Jenkins, R. D.; Winnik, M. A.; Bassett, D. R. *Macromolecules* **1998**, *31*, 4149.
(14) Wientjes, R. H. W.; Jongschaap, R. J. J.; Duits, M. H. G.; Mellema, J. *J. Rheol.* **1999**, *43*, 375.
(15) Serero, Y.; Jacobsen, V.; Berret, J. F.; May, R. *Macromolecules* **2000**, *33*, 1841.
(16) Yao, N.; Jamieson, A. M. *Polymer* **2000**, *41*, 2925.
(17) Folmer, B. J. B.; Sijbesma, R. P.; Versteegen, R. M.; van der Rijt, J. A. J.; Meijer, E. W. *Adv. Mater.* **2000**, *12*, 874.
(18) Glass, J. E. *J. Coating Technol.* **2001**, *73 (Feb)*, 79.
(19) Berret, J. F.; Serero, Y. *Phys. Rev. Lett.* **2001**, *8704*, 8303.
(20) Kumar, S. K.; Douglas, J. F. *Phys. Rev. Lett.* **2000**, *8718*, 8301.
(21) Stadler, R.; Freitas, L. D. *Colloid Polym. Sci.* **1986**, *264*, 773.
(22) Muller, M.; Kremer, F.; Stadler, R.; Fischer, E. W.; Seidel, U. *Colloid Polym. Sci.* **1995**, *273*, 38.
(23) Muller, M.; Stadler, R.; Kremer, F.; Williams, G. *Macromolecules* **1995**, *28*, 6942.
(24) Klok, H. A. Rebrov, E. A.; Mauzafarov, A. M.; Michelberger, W.; Moller, M. *J. Polym. Sci. Part B: Polym. Phys.* **1999**, *37*, 485.
(25) Hirschberg, J. H. K. K.; Beijer, F. H.; van Aert, H. A.; Magusim, P. C. M. M.; Sijbesma, R. P.; Meijer, E. W. *Macromolecules* **1999**, *32*, 2696.
(26) Jackson, C. L.; McKenna, G. B. *J. Non-Cryst. Solids* **1991**, *131−133*, 221.
(27) Kremer, F.; Huwe, A.; Arndt, M.; Behrens, P.; Schweiger, W. *J. Phys. Condens. Matter* **1999**, *11*, A175.
(28) Huwe, A.; Kremer, F.; Behrens, P.; Schweiger, W. *Phys. Rev. Lett.* **1999**, *82*, 2338.
(29) Schonhals, A.; Stauga, R. *J. Chem. Phys.* **1998**, *108*, 5130.
(30) Anastasiadis, S. H.; Karatasos, K.; Vlachos, G.; Manias, E.; Giannelis, E. P. *Phys. Rev. Lett.* **2000**, *84*, 915.
(31) Reiter, G. *Europhys. Lett.* **1993**, *23*, 579.
(32) Keddie, J. L.; Jones, R. A. L.; Cory, R. A. *Europhys. Lett.* **1994**, *27*, 59.
(33) Kawana, S.; Jones, R. A. L. *Phys. Rev. E* **2001**, *63*, 1501.
(34) Prucker, O.; Christian, S.; Bock, S.; Ruhe, J.; Frank, C. W.; Knoll, W. *Macromol. Chem. Phys.* **1998**, *199*, 1435.
(35) Pochan, D. J.; Lin, E. K.; Satija, S. K.; Wu, W.-L. *Macromolecules* **2001**, *34*, 3041.
(36) van Zanten, J. H.; Wallace, W. E.; Wu, W.-L. *Phys. Rev. E* **1996**, *53*, R2053.
(37) Schwab, A. D.; Agra, D. M. G.; Kim, J.-H.; Kumar, S.; Dhinojwala, A. *Macromolecules* **2000**, *33*, 4903.
(38) Tsui, O. K. C.; Russell, T. P.; Hawker, C. J. *Macromolecules* **2001**, *34*, 5535.
(39) Ellison, C. J.; Kim, S. D.; Torkelson, J. M. *Eur. Phys. J. E*, in press.
(40) Forrest, J. A.; Dalnoki-Veress, K.; Stevens, J. R.; Dutcher, J. R. *Phys. Rev. Lett.* **1996**, *77*, 2002.
(41) Forrest, J. A.; Dalnoki-Veress, K.; Dutcher, J. R. *Phys. Rev. E* **1998**, *58*, 6109.
(42) Hall, D. B.; Hooker, J. C.; Torkelson, J. M. *Macromolecules* **1997**, *30*, 667.
(43) Fukao, K.; Miyamoto, Y. *Phys. Rev. E* **2000**, *61*, 1743.
(44) Daoukaki, D.; Barut, G.; Pelster, R.; Nimtz, G.; Kyritsis, A.; Pissis, P. *Phys. Rev. B* **1998**, *58*, 5336.
(45) Newby, B. M. Z.; Composto, R. J. *Macromolecules* **2000**, *33*, 3274.
(46) Zhu, S.; Liu, Y.; Rafailovich, M. H.; Sokolov, J.; Gersappe, D.; Winesett, D. A.; Ade, H. *Nature* **1999**, *400*, 49.
(47) Dalnoki-Veress, K.; Forrest, J. A.; Dutcher, J. R. *Phys. Rev. E* **1998**, *57*, 5811.
(48) Kim, S. D.; Torkelson, J. M. Manuscript in preparation; *Polym. Mater. Sci. Eng.* **2001**, *85*, 2.
(49) Ruths, M.; Granick, S. *J. Phys. Chem. B* **1999**, *103*, 8711.
(50) Kuznetsov, D. V.; Balazs, A. C. *J. Chem. Phys.* **2000**, *113*, 2479.
(51) Kane, M. A.; Baker, G. A.; Pandey, S.; Maziarz, E. P.; Hoth, D. C.; Bright, F. V. *J. Phys. Chem. B* **2000**, *104*, 8585.
(52) Kane, M. A.; Pandey, S.; Baker, G. A. Perez, S. A.; Bukowski, E. J.; Hoth, D. C.; Bright, F. V. *Macromolecules* **2001**, *34*, 6831.
(53) Char, K.; Gast, A. P.; Frank, C. W. *Langmuir* **1988**, *4*, 989.
(54) Char, K.; Frank, C. W.; Gast, A. P.; Tang, W. T. *Macromolecules* **1987**, *20*, 1833.
(55) Lee, S.; Duhamel, J. *Macromolecules* **1998**, *31*, 9193.
(56) Kelly, M. S.; Santore, M. M. *J. Appl. Polym. Sci.* **1995**, *58*, 247.
(57) Duhamel, J.; Yekta, A.; Hu, Y. Z.; Winnik, M. A. *Macromolecules* **1992**, *25*, 7024.
(58) Ezzell, S. A.; McCormick, C. L. *Macromolecules* **1992**, *25*, 1881.
(59) Ezzell, S. A.; Hoyle, C. E.; Creed, D.; McCormick, C. L. *Macromolecules* **1992**, *25*, 1887.
(60) Kosbar, L. L.; Frank, C. W. *Polymer* **1992**, *33*, 141.
(61) Richey, B.; Kirk, A. B.; Eisenhart, E. K.; Fitzwater, S.; Hook, J. *J. Coating Technol.* **1991**, *63*, 31.
(62) Prazeres, T. J. V.; Beingessner, R.; Duhamel, J.; Oleson, K.; Shay, G.; Bassett, D. R. *Macromolecules* **2001**, *34*, 7876.
(63) Major, M. D.; Torkelson, J. M.; Brearley, A. M. *Macromolecules* **1990**, *23*, 1700.
(64) Major, M. D.; Torkelson, J. M.; Brearley, A. M. *Macromolecules* **1990**, *23*, 1711.
(65) Hall, D. B.; Underhill, P.; Torkelson, J. M. *Polym. Eng. Sci.* **1998**, *38*, 2039.
(66) Hall, D. B.; Miller, R. D.; Torkelson, J. M. *J. Polym. Sci. Part B Polym. Phys.* **1997**, *35*, 2795.

(67) Svirskaya, P.; Danhelka, J.; Redpath, A. E. C.; Winnik, M. A. *Polymer* **1983**, *24*, 319.
(68) Schillen, K.; Anghel, D. F.; Miguel., M. D. G.; Lindman, B. *Langmuir* **2000**, *16*, 10528.
(69) Winnik, F. M. *Chem. Rev.* **1993**, *93*, 587.
(70) Oyama, H. T.; Hemker, D. J.; Frank, C. W. *Macromolecules* **1989**, *22*, 1255.
(71) Farinha, J. P. S.; Martinho, J. M. G.; Xu, H.; Winnik, M. A.; Quirk, R. P. *J. Polym. Sci. Part B Polym. Phys.* **1994**, *32*, 1635.
(72) Daoud, M.; Jannink, G. *J. Phys. Paris* **1976**, *37*, 973.
(73) Torkelson, J. M.; Gilbert, S. R. *Macromolecules* **1987**, *20*, 1860.
(74) Buyuktanir, E. A.; Kucukyavuz, Z. *J. Polym. Sci. Part B Polym. Phys.* **2000**, *38*, 2678.
(75) Ellison, C. J.; Kim, S. D.; Torkelson, J. M. Manuscript in preparation.
(76) Jones, R. A. L. *Curr. Opin. Colloid Interfact Sci.* **1999**, *4*, 153.
(77) From simple arguments, $a = 2h_I[K_{EI}/K_{MB} - K_{EB}/K_{MB}] = 2h_I[(K_{EI}/K_{EB})(K_{EB}/K_{MB}) - K_{EB}/K_{MB}] = 2h_I(K_{EB}/K_{MB})(K_{EI}/K_{EB} - 1)$, where K_{EB}/K_{MB} can be obtained from the nonlinear fit or experimental data in thick films above 200 nm. Note that K is a proportionality constant and is equal to intensity divided by film thickness. K_{EI}/K_{EB} can be obtained from data in Figure 8.
(78) Guilbault, G. G. In *Practical Fluorescence*, 2nd ed.; Marcel Dekker: New York, 1990; p 28.
(79) Robertson, J. M.; White, J. W. *J. Chem. Soc.* **1947**, 358.
(80) Brown, T. L.; LeMay, H. E.; Bursten, B. E. In *Chemistry: The Central Science*; Prentice Hall: Englewood Cliffs, NJ, 1994.
(81) Hall, D. B.; Hamilton, K. E.; Miller, R. D.; Torkelson, J. M. *Macromolecules* **1999**, *32*, 8052.
(82) Lantz, M. A.; Jarvis, S. P.; Tokumoto, H.; Marynski, T.; Kusumi, T. Nakamura, C.; Miyake, J. *Chem. Phys. Lett.* **1999**, *315*, 61.
(83) Rubinstein, M.; Semenov, A. N. *Macromolecules* **1998**, *37*, 1386.

MA0200322